euronoise

Performances of a multi-static model of sound scattering by rough surfaces

Virginie Jaud, Cédric Gervaise and Ali Khenchaf

E3I2 - EA3876, 2 rue François Verny, 29806 Brest Cedex, France
virginie.jaud@ensieta.fr

The ocean floor is far from being a smooth and perfectly rigid surface. That is why its sound scattering properties are a useful input to the analysis of this medium as for acoustic data inversion. Thus, scattering strength has been investigated at high frequency of order of 10kHz to hundreds of kHz under different geometrical configurations. The Kirchhoff Approximation and the Small Perturbation Method could be cited respectively in the case of dimensions of a rough surface larger and smaller than the wavelength. Nevertheless, modeling a rough surface should be considered at different scales compared to the wavelength. As a part of the incident wave is transmitted to the seabed medium, it is also important to know the effect of the scattering coming from the volume. Jackson's scattering model takes these considerations into account. The aim of our study is first to show an improvement of the surface scattering method using the Small Slope Approximation and keeping the initial method of Jackson's model to describe the scattering from the volume. Comparisons with a well-known model are presented to show the performances of this new approach and comparisons between different geometries are analyzed to show the most useful configurations of the model.

1 Introduction

Acoustic scattering from ocean bottom is a subject of interest to the underwater acoustic community. Different studies have been carried out considering the complexity of the ocean bottom. This complex acoustic medium may be assumed as elastic-solid, fluid or porous to solve scattering problem. These assumptions make the models have different limitations. In this paper, the models deal with sound waves at high frequencies for a scattering fluid(water)-fluid(seafloor) interface with a rough surface between both media. The roughness scattering is predicted with the Small Slope Approximation (SSA) which was first developed by Voronovich [8]. The inhomogeneities in the sediment are analyzed as volume scattering with a model first formulated by Mourad and Jackson [7] for a backscattering configuration and then generalized for the bi-static case [2]. A full process is described as the sum of both components, the roughness scattering and the volume scattering. In particular cases, the roughness scattering level is higher than the volume scattering, thus the total scattering is said to result from the roughness of the surface. For other situations, the volume scattering effect is greater than the roughness effect or may be more or less similar to the roughness scattering component. These different situations depend on the media, the frequency of the emitted wave, the angles of the incident and scattered waves, and so on. We are more interested by the roughness scattering even if volume scattering must be included in the scattering implementation to reach a valuable model. For the sake of simplicity, this full process is called "SSA-volume" and is the sum of roughness and volume scattering strength components.
In this paper, the Small Slope Approximation of first order is shown to be pertinent enough to replace the roughness scattering theory used in the bi-static model developed in [2, 4] and called "Jackson's model". The volume scattering component of SSA-volume model is similar to the one implemented in Jackson's model. In Jackson's model, roughness scattering strength is predicted by an interpolation of the Kirchhoff Approximation (KA) and the Small Perturbation Method (SPM). KA is used to evaluate scattering strength in the specular directions, whereas SPM is used for predictions in other directions than the specular one and works well with a roughness relief smaller than the acoustic wave length. Small Slope Approximation has been elaborated as an unifying method that could reconcile SPM and KA without separating the spectrum of the rough surface into large and small deviations of the relief. The validity condition of this method consists only in the smallness of the elevation slopes, without any restriction on the sound wavelength which is a limitation for the other scattering models.
In Section 2, the scattering problem is described in terms of incident and scattered waves. The environment where the process takes place plays a crucial role in the scattering analysis and is briefly presented as well as the theory of the SSA-volume model. Then a simulation study is carried out in Section 3. Scattering strength is expressed for the scattering case in one plane which is a special case of the bi-static configuration. Next, the azimuth angle of the scattered angles is changed to get a global view over the configuration. The scattering predictions are discussed in Section 4.
The use of SSA for predicting roughness scattering works well and perspectives about this method are clear as the possible use of it with a more complicated rough interface. Finally, the aim of this study is first to show that SSA performs as well as the roughness predictions of Jackson's model under similar configurations. Then, SSA can be suitable to many fluid environments with more complex roughness than the one used in this paper. This would be out of the limits where Jackson's model is applicable. Those predictions should be presented in a future paper under its full process, SSA-volume, to reach as closer as possible the reality of different seabeds.

2 Background

The geometry of the scattering problem is depicted in Figure 1 in terms of incident and scattered sound waves. $\mathbf{k_i}$ and $\mathbf{k_s}$ represent respectively the incident and scat-

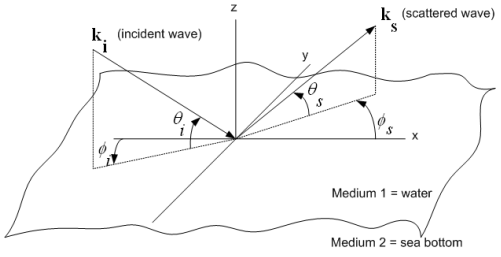

Figure 1: Geometry of the scattering problem.

tered wave vectors.

$$\mathbf{k_i} = \{\mathbf{K_i}, -k_{zi}\}, \qquad \mathbf{k_s} = \{\mathbf{K_s}, k_{zs}\} \tag{1}$$

where $\mathbf{K_i}$, $\mathbf{K_s}$ are the transverse components of the incident and scattered waves in the (x, y) directions, so $\mathbf{K_i} = \{k_{xi}, k_{yi}\}$ and $\mathbf{K_s} = \{k_{xs}, k_{ys}\}$. The vertical components in the z-direction, k_{zi} and k_{zs}, respect $k_z = \sqrt{k^2 - (k_x^2 + k_y^2)}$, with k the wavenumber. Notice that the scattering theory depends on the grazing angles θ_i, θ_s and the azimuth angles ϕ_i and ϕ_s. The scattering process depends also on the parameters of the media where sound scattering takes place. Medium 1 is the water. Its sound velocity is assumed to be constant with $c_1 = 1500m/s$ and to have a mass density equals to $\rho_1 = 1000kg/m^3$. Medium 2 is described by many parameters related to the roughness and the inhomogeneities of the seafloor. This set of data is found in Table 1. This has been established for different seafloors and they are found in [3, 4, 5].

Symbol	Definition
ρ	Density ratio (ρ_2/ρ_1)
ν	Sound speed ratio (c_2/c_1)
δ	Loss parameter
w_2	Roughness spectral strength
γ_2	Rough spectral exponent
w_3	Volume spectral strength
γ_3	Volume spectral exponent
μ	Fluctuation ratio

Table 1: Seafloor parameters

2.1 Modeling a rough interface

A rough interface separates the two fluid media. This surface is considered plane on the average and is defined as:

$$z = h(\mathbf{r}) \tag{2}$$

where $\mathbf{r} = (x, y)$ is the position on the x-y-plane, h is the deviation of the interface relative to its means plane $z = 0$. One way to represent the roughness of a surface is the relief structure function. Notice that the structure function can be connected to the spectrum of the surface, W, in case of this component is needed for instance in a data inversion process [1].

$$D(\mathbf{r}) = 2\int_{-\infty}^{+\infty}\int_{-\infty}^{+\infty}(1 - \cos(\mathbf{K}\cdot\mathbf{r}))\,W(\mathbf{K})d\mathbf{K} \tag{3}$$

The structure function of the rough surface is defined as $D(\mathbf{r}) =< [h(\mathbf{r}+\mathbf{r_0}) - h(\mathbf{r_0})]^2 >$ where $h(\mathbf{r})$ is the elevation at the position $\mathbf{r} = \{x, y\}$ and $h(\mathbf{r}_0)$ the elevation at the origin. The structure function is also related to the covariance $B(\mathbf{r})$ as twice the difference between the covariance at the origin and the one at the position $\mathbf{r}$:

$$D(\mathbf{r}) = 2(B(0) - B(\mathbf{r})) \tag{4}$$

In this paper, the surface is supposed to be isotropic, so the structure function depends only on the magnitude r of the two-dimensional vector $\mathbf{r}$. In a future paper, this simplification will not be applied to see performances of such complicated case. To be comparable with the bistatic model proposed in [2, 4], the structure function is defined as:

$$D(r) = C_h^2 r^{2\alpha} \tag{5}$$

where

$$C_h^2 = \frac{2\pi w_2 \Gamma(2-\alpha)2^{-2\alpha}}{\alpha(1-\alpha)\Gamma(1+\alpha)}, \qquad \alpha = (\gamma_2/2) - 1 \tag{6}$$

where γ_2 is the spectral exponent. For such a structure function, the related two-dimensional roughness spectrum is expressed as $W(\mathbf{K}) = w_2/K^{\gamma 2}$ where $\mathbf{K}$ is the related two-dimensional wave vector, K the amplitude of $\mathbf{K}$ and w_2 the spectral strength. In underwater Acoustics, this spectral shape is typical for representing the roughness of a surface.

2.2 Modeling acoustic scattering: a brief outline of theory

The scattering strength, S, predicted in Section 3 is defined in decibel (dB) as:

$$\begin{aligned} S(\theta_i, \phi_i, \theta_s, \phi_s) &= 10\log_{10}[\sigma_r(\theta_i, \phi_i, \theta_s, \phi_s) \\ &+ \sigma_v(\theta_i, \phi_i, \theta_s, \phi_s)] \end{aligned} \tag{7}$$

where $\sigma_r(\theta_i, \phi_i, \theta_s, \phi_s)$ is the roughness contribution and $\sigma_v(\theta_i, \phi_i, \theta_s, \phi_s)$ the volume contribution to the scattering cross section per unit area. $\sigma_r(\theta_i, \phi_i, \theta_s, \phi_s)$ is evaluated with the Small Slope Approximation at first order and is expressed as:

$$\begin{aligned} &\sigma_r(\theta_i, \phi_i, \theta_s, \phi_s) = \frac{|A_{spm}(\theta_i, \phi_i, \theta_s, \phi_s)|^2}{2\pi(k_{zs} + k_{zi})^2} \\ &\times \int_0^\infty \left(e^{\left[(k_{zs}+k_{zi})^2 D(\mathbf{r})\right]} - e^{\left[(k_{zs}+k_{zi})^2 D(\infty)\right]}\right) \\ &\times e^{(-i(\mathbf{K_s}-\mathbf{K_i})\cdot\mathbf{r})} d\mathbf{r} \end{aligned} \tag{8}$$

where D is the structure function, k_{zi}, k_{zs}, $\mathbf{K_i}$ and $\mathbf{K_s}$ are the wave vector components defined before in Section 2. Notice that the rough surface is considered as isotropic and this allowed the integral of Eq(8) to be simplified. The roughness scattering component is finally:

$$\begin{aligned} &\sigma_r(\theta_i, \phi_i, \theta_s, \phi_s) = \frac{|A_{spm}(\theta_i, \phi_i, \theta_s, \phi_s)|^2}{2\pi(k_{zs} + k_{zi})^2} \\ &\times \int_0^\infty \left(e^{\left[(k_{zs}+k_{zi})^2 D(\mathbf{r})\right]} - e^{\left[(k_{zs}+k_{zi})^2 D(\infty)\right]}\right) J_0(Qr) r dr \end{aligned} \tag{9}$$

where J_0 is the zeroth-order Bessel function of the first kind, Q is the magnitude of the transverse component difference modified [5] to prevent numerical difficulties as:

$$Q = \sqrt{(k_{xs} - k_{xi})^2 + (k_{ys} - k_{yi})^2 + (k \times 0.001)^2} \tag{10}$$

A_{spm} is a coefficient which depends on the properties of the lower medium and is obtained using first-oder perturbation theory for the corresponding problem. For a fluid-fluid multi-static problem, this component is defined as:

$$\begin{aligned} &|\, A_{spm}(\theta_i, \phi_i, \theta_s, \phi_s)|^2 = \frac{k^4}{4} \\ &\times \quad |\,[\Gamma(\theta_s) + 1]\,[\Gamma(\theta_i) + 1]\,|^2 \\ &\times \quad \left|\, 1 + \frac{\kappa^2}{\rho} + \left(\frac{1}{\rho} - 1\right)^2 \left(\frac{\mathbf{K_s}\cdot\mathbf{K_i}}{k^2} - \frac{P_g^2(\theta_i,\theta_s)}{\rho}\right) \right|^2 \end{aligned} \tag{11}$$

where $\rho = \rho_2/\rho_1$, $\kappa = k_2/k_1 = c_1/c_2$, $k = 2\pi f/c_1$ with f the frequency of the incident plane wave. $\Gamma(\theta)$ is the plane-wave reflection coefficient and P_g^2 is equivalent to the expression [6]:

$$P_g^2(\theta_i, \theta_s) = \rho^2 \sin(\theta_s)\sin(\theta_i) \times \left(\frac{1-\Gamma(\theta_s)}{1+\Gamma(\theta_s)}\right)\left(\frac{1-\Gamma(\theta_i)}{1+\Gamma(\theta_i)}\right) \quad (12)$$

Once the roughness contribution is established, the volume scattering is briefly described and corresponds to the component used in [2, 4]:

$$\sigma_v(\theta_i, \phi_i, \theta_i, \phi_s) = \frac{|1+\Gamma(\theta_i)|^2|1+\Gamma(\theta_s)|^2\sigma_{pm}}{2k\rho^2 Im\left[P(\theta_i)+P(\theta_s)\right]} \quad (13)$$

σ_{pm} is the coefficient obtained by the perturbation method and adapted by [2] as:

$$\sigma_{pm} = \frac{\pi}{2}k^4|\mu\kappa^2 + \cos\theta_i\cos\theta_s\cos(\phi_s-\phi_i) - P(\theta_i)P(\theta_s)|^2 W_{\rho\rho}(\Delta k) \quad (14)$$

$W_{\rho\rho}(\Delta k)$ is the spectrum for density fluctuation,

$$W_{\rho\rho}(\Delta k) = w_3/(\Delta k)^{\gamma 3} \quad (15)$$

evaluated at the Bragg wave number, thus Δk is the magnitude difference between the real part of the incident and the scattered three dimensional wave vectors.

$$\Delta k = k|4Q^2 + (Re\left[P(\theta_i)+P(\theta_s)\right])^2|^{1/2} \quad (16)$$

Note that acoustic loss is taken into account in the volume scattering coefficient by allowing the wave number in the seabed to be complex. $P(\theta) = \sqrt{\kappa^2 - \cos(\theta)^2}$ is the complex wave number in the sediment divided by the real wave number in the water.
The main components have been described for simulating SSA-volume model. The comparison with the well-known Jackson's model has been done thanks to the expressions coming mainly from [4].

3 A simulation study

A simulation study has been carried out with different configurations. Scattering strength predictions are made from SSA-volume. Four types of seafloor are considered in this paper which are silt, medium sand, coarse sand and sandy gravel. Parameters describing those floors are given in Table 2. These different kinds of seafloor make the relief have many dimensions, different sound absorption effects, and so on. Notice that those media can be assumed as fluid media where only the compressional wave is of importance. This would not be possible with a rock medium where shear waves are also very noticeable compared to compressional waves. All plots represent the scattering strength predicted from SSA-volume model compared to Jackson's model, except Figure 3 which shows the prediction of scattering strength from SSA-volume model, the prediction of roughness scattering from SSA and the volume scattering effect. The purpose of Figure 3 is to see whether our study of roughness scattering is pertinent in the global scattering process.

Bottom Properties	Types of seafloor			
	sandy gravel	coarse sand	medium sand	silt
ρ	2.492	2.231	1.845	1.149
μ	1.337	1.2503	1.1782	0.9873
δ	0.01705	0.01638	0.01624	0.00386
γ_2	3	3.25	3.25	3.25
w_2	0.00018	0.00022	0.0001406	0.0000165
γ_3	3	3	3	3
w_3	0.000377	0.000362	0.000359	0.00004269

Table 2: Properties of many seafloors (from [5])

3.1 Scattering in one plane

In the first test case, the seafloor is made of sandy gravel and has the properties described in Table 2. The incident plane wave has a frequency of 30kHz, a grazing angle $\theta_i = 10°$ first. Next θ_i is set to 40°. The geometrical configuration is in one plane, thus $\phi_s = \phi_i = 0°$. Figure 2 shows the predicted scattering strength as function of θ_s. Figure 2 shows clearly a maximum of scatter-

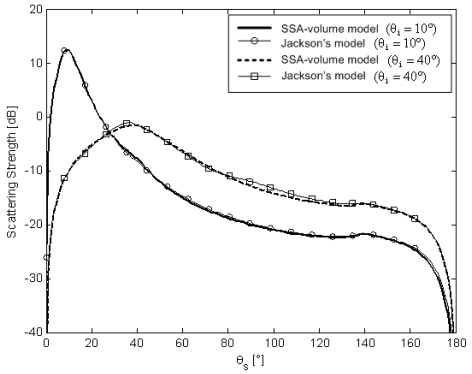

Figure 2: Scattering strength as function of θ_s, for $\theta_i = 10°$ and $\theta_i = 40°$, $\phi_i = \phi_s = 0°$, f=30kHz, with a sandy gravel seafloor.

ing energy for each case. Those maxima represent the energy scattered in the specular direction, i.e. around $\theta_s = 10°$ for the configuration with $\theta_i = 10°$ and around $\theta_s = 40°$ for the configuration with $\theta_i = 40°$. The maximum value is also different between configurations because the transmission, reflection, and so the scattering processes depend on the angles of the incident and scattered waves. Notice that predictions provided by SSA-volume model and Jackson's model are similar with a slight difference, less than 1dB, around $\theta_s = 100°$ for the configuration with $\theta_i = 40°$.
In a second case, two types of seafloor are used, one made of sandy gravel and the other one of a softer texture with silt. The incident grazing angle of the 30kHz-plane wave is $\theta_i = 10°$ in the plane ($\phi_s = \phi_i = 0°$) and is as function of θ_s. In case of a silty seafloor, the volume scattering effect is greater than the roughness scattering, whereas the roughness scattering is dominant compared to the volume scattering in case of a sandy gravel seafloor. The study of roughness scattering strength versus volume scattering has already been done [3] under different considerations. The prediction presented in Figure 3 shows that the study of SSA in a global model is pertinent only if the roughness scatter-

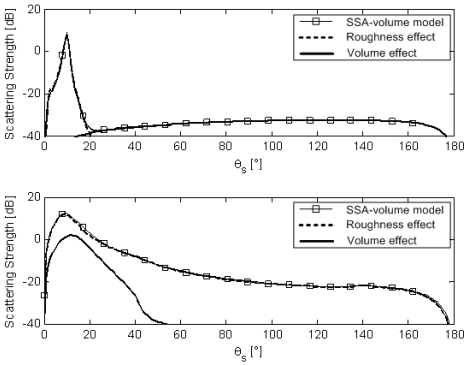

Figure 3: Effects of volume and roughness scattering as function of θ_s, for $\theta_i = 10°$, $\phi_i = \phi_s = 0°$, f=30kHz, top:silt; bottom:sandy gravel.

ing is more noticeable than the volume scattering.
A third case is analyzed here with two different frequencies, 10kHz and 100kHz. Those frequencies represent the minimum and the maximum of the frequency band where Jackson's model is said to be applicable. Comparisons are made between SSA-volume model and Jackson's model in Figure 4. Similar test cases have

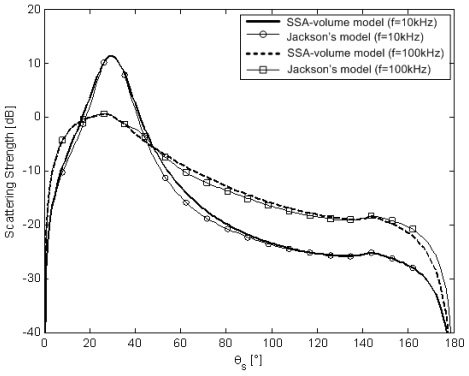

Figure 4: Scattering strength as function of θ_s, for $\theta_i = 30°$, $\phi_i = \phi_s = 0°$, f=10kHz and f=100kHz, with a coarse sand as bottom.

been examined with many kinds of seafloor and many frequencies being higher than 100kHz. Slight differences, less than 1-2dB, between the predictions from SSA-volume and Jackson'model appear around $\theta_s = 80°$ and $\theta_s = 170°$ for the configuration at f=100kHz, and around $\theta_s = 30°$ and $\theta_s = 60°$ for the configuration at f=10kHz. The slight differences around the specular direction correspond to the position where the connection is done between KA and SPM in Jackson's model.

3.2 Sound source and receiver in different planes

Simulations are performed with configurations where the azimuth scattered angle ϕ_s changes. Figure 5 shows the scattering strength in a case of an incident plane wave at 30kHz emitted with a set of angles $\theta_i = 40°$ and $\phi_i = 0°$. The scattering is predicted with an azimuth angle $\phi_s = 45°$ first (top of Figure 5) and then with $\phi_s = 135°$ (bottom of Figure 5). Scattering strength is showed as function of the scattered angle θ_s. Two types of seafloor are considered, a sandy gravel medium and a coarse sand medium. The scattering strength predic-

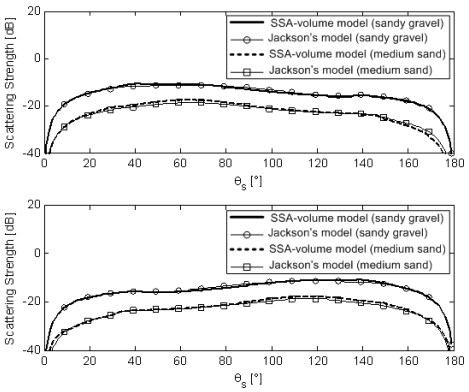

Figure 5: Scattering strength as function of θ_s, for $\theta_i = 40°$, $\phi_i = 0$, f=30kHz, top: $\phi_s = 45°$; bottom: $\phi_s = 135°$.

tions of SSA-volume model are similar for the different seafloor and for the two azimuth scattered angles that have been simulated compared to Jackson'model. The maximum energy observed with a clear peak in the previous cases is not seen here in Figure 5.
Figure 6 shows scattering strength as function of the scattered azimuth angle ϕ_s. The incident plane wave is set to $\theta_i = 15°$ and $\phi_i = 0°$. The scattered grazing angle is equal to the incident grazing angle, i.e. $\theta_s = 15°$. Those angles make the plane waves be close to the horizontal plane. The results are predicted with sandy gravel first and then with medium sand. The predic-

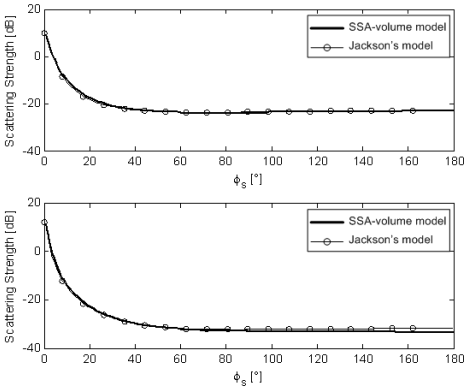

Figure 6: Scattering strength as function of ϕ_s, for $\theta_i = \theta_s = 15°$, $\phi_i = 0°$, f=30kHz, top: sandy gravel; bottom: medium sand.

tion with both models are still similar, except for the case with a medium sand seafloor. A slight difference, less than 2dB, is seen in the backward direction between $\phi_s = 100°$ and $\phi_s = 180°$. Strength at $\phi_s = 0$ represents the energy in the specular direction.
Figure 7 shows scattering strength as function of the azimuth angle ϕ_s for a set of angles $\theta_i = \theta_s = 40°$ and $\phi_i = 0$. The prediction of the volume scattering is also plotted. The seafloor is made of medium sand. Scattering strength predictions are shown for two frequencies at 10kHz and 200kHz. Strength around $\phi_s = 0°$ is higher for the configuration f=10kHz (top of Figure 7) than the

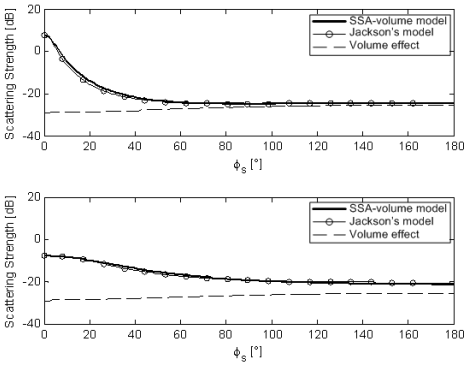

Figure 7: Scattering strength for a medium sand seafloor as function of ϕ_s, for $\theta_i = \theta_s = 40°$, $\phi_i = 0°$, top: f=10kHz; bottom: f=200kHz.

one for the configuration with f=200kHz (bottom of Figure 7). At different frequencies, a surface is more or less rough. Higher the frequency is, rougher a sandy seafloor is. That is why the energy in the specular direction is lower for higher frequencies. Notice that the volume scattering effect is less and less noticeable when the frequency increases. Low frequency waves penetrate into a medium more than high frequency waves for a given seafloor. Thus plane waves with higher frequencies are less affected by volume scattering.

4 Discussion

SSA-volume model predicts basically the same scattering strength as the Jackson's model does in its limits of predictions. SSA is an unified method, whereas the roughness component of Jackson's model is the interpolation of both methods KA and SPM. Scattering predictions with SSA in the specular direction are well done as the predictions in the scattered direction, without restriction on grazing angles. SPM is used for predicting away from the specular direction and is limited to small surface roughness, whereas SSA is not restricted to this type of surface. There is no need of a cross section between a method for prediction in the specular direction and another in the scattered direction. Models which are based on the connection between two models as Jackson's model, can meet limitations if both KA and SPM data does not cross each other during their connection. Another point should be mentioned. Jackson's model is used here under a multi-static form. Its backscattering version exists and is based on KA and the Two Scale Model. Despite the fact that this version has not been written with a multi-static geometry, this takes multi-roughness into account as SSA does. Furthermore, SSA works well for many configurations and this would be of importance when the surface is not isotropic. The few differences (less than 2 dB) seen between predictions of SSA-volume and Jackson'model correspond to angles where KA and SPM meet and at extreme grazing angle in certain cases. Notice that the integral of SSA has been numerically solved and the way to solve it may be more or less complicated depending on the scattering problem. SSA-volume model performed well for isotropic surface with different dimensions and is attended to perform for anisotropic sandy surface as sandy ripples which got directional spectrum. Our simulations confirm that the use of SSA is of interest only if the roughness scattering strength is greater than the volume scattering. Predictions of scattering for a seafloor going from fine sand to sandy gravel seem to be relevant since the scattering volume is still less important than the roughness scattering. Moreover the rougher surface that has been studied still makes the sound waves be only compressional and shear waves are avoided.

5 Conclusion

Predictions of roughness scattering can be based on Small Slope Approximation, combined to a volume scattering prediction model to cope with existing scattering problems. In this paper, an isotropic interface is assumed and a simplified expression of SSA results from this surface behavior. The change of such surface by one with a directional spectrum would make the numerical integral in SSA more complicated to solve but the predictions would be of importance. Another perspective would be to predict roughness instead of roughness scattering via the structure function by extraction of this component from the expression of SSA.

References

[1] D.R Jackson, D.P.Winebrenner, A.Ishimaru, "Application of the composite roughness model to high-frequency bottom backscattering", *J. Acoust. Soc. Am. 79*, 1410-1422 (1986)

[2] D.R Jackson, "A bistatic bottom scattering: Model, experiments, and model/data comparison", *J. Acoust. Soc. Am. 103*, 169-181 (1997)

[3] D.R Jackson, K.B.Briggs, "High-frequency bottom backscattering: Roughness versus sediment volume scattering", *J. Acoust. Soc. Am. 92*, 962-977 (1992)

[4] D.R Jackson, "APL-UW High Frequency Ocean Environmental Acoustic Models Handbook", *Applied Physics Laboratory, University of Washington, Technical report 9407* (October 1997)

[5] D.R Jackson, "APL-UW High-Frequency Bistatic Scattering Model for Elastic Seafloors", *Applied Physics Laboratory, University of Washington, Technical report 2-00* (February 2000)

[6] J.E.Moe, D.R Jackson, "First-order perturbation solution for rough surface scattering cross section including the effects of gradients", *J. Acoust. Soc. Am. 96*, 1748-1754 (1994)

[7] P.D.Mourad, D.R Jackson, "High frequency sonar equation models for bottom backscatter and forward loss", *Proceedings of OCEANS'89*, 1168-1175 (1989)

[8] A.G. Voronovich, "Wave scattering from rough surfaces", *Springer Series on Wave Phenomena, Second updated edition*, (1998)